Project Number: <ME-SPN-AB1M>

Design for Additive Manufacturing – An Integrated Robot Frame and Hydraulic Manifold

A Major Qualifying Project Report

Submitted to the Faculty

of the

WORCESTER POLYTECHNIC INSTITUTE

in partial fulfillment of the requirements for the

Degree of Bachelor of Science

in Mechanical Engineering

by

Travis Wold

Date: May 2020

Prof. Sneha. P. Narra, MQP Advisor

Table of Contents

List of Figures

List of Tables

Introduction

Over 250 years ago, new manufacturing processes led to a period known as the First Industrial Revolution. Within the last few decades, the introduction of 3D printing has enabled innovation in design for manufacture; complex, one-off shapes can be produced in relatively short lead times. Additive manufacturing (AM) is the start of the next industrial revolution if designers learn to fully exploit its capabilities. Replacing existing parts with AM parts has some benefits in production and further component adaptation leads to weight, cost, and performance advantages. However, additive manufacturing will not disrupt or revolutionize industrial manufacturing until we can design the parts specifically with AM in mind. Design for additive manufacturing not only requires the designer or engineer starts from a clean slate in part realization, but also considers the buildability and economics of the component from the beginning as well.

Literature Review

There are two important areas of interest when designing a part for additive manufacturing. First, what print method and materials are best suited for the component being redesigned. Second, what are the existing designs, their limitations, and the latest developments in the manufacture of these designs.

Additive Manufacturing

Additive manufacturing is a disruptive technology, not only because it has the capability of revolutionizing the ways of production, but also because additive manufacturing enables designers to realize completely new products which were impossible to produce using subtractive manufacturing.

The wide variety of additive manufacturing (AM) processes are all classified by their mechanism to add a metallic powder, layer by layer, to the part's surface [1]. In the end a 3-dimensional part is produced near its final shape before any traditional subtractive manufacturing techniques such as milling, turning, etc. First, we distinguish systems that partially melt the metallic powder from those which fully melt the powder. The next distinguishing feature is the method by which the power is fed to the system. The part may either be produced within a bed of metallic powder and after each pass of a laser, a new layer is spread over top. Another method sprays the powder directly into the melt pool on the part. Finally, there are many proprietary systems within these, some of which designed for processing a specific material though following the same principles.

The first category is known Laser Sintering (LS) [1]. This implies that rather than fully melting the powder as the other AM machines do, a LS machine will sinter the particles together so that the part resembles its final shape. Often, a binder material distinct from the structural material is used for its lower melting temperature to join the larger structural particles together. LS is also capable of combining pre-alloyed powders. However, these must transition from melt to solid through the semi-solid "mushy" zone. The greater the change in temperature between the complete liquid to complete solid, the greater the likelihood for warping and cracking. These residual stresses most often need to be relieved either through a high temperature post-sintering process or hot isostatic pressing (HIP).

Developments in laser technologies have enabled the complete melting of the powder, thereby producing fully dense (99.9%) parts without the need for post-sintering or HIP [1]. Higher laser power, smaller laser focus, and smaller layer height all contribute to improvements in smoothness, microstructure, and densification of Laser Melting (LM) and Laser Metal Deposition (LMD) machines. The distinguishing

characteristic between these two types of machines is their method of feeding powder to the system. LM machines are constructed in the same way as LS machines. Both contain a bed of powder which is scanned with a laser, then recovered with another layer of powder, each time bonding to the layer below, finally producing a part when all the layers have been melted or sintered together. However, the smaller laser focus and so smaller layer height results in longer build times with LM machines. LMD machines have no powder bed. Instead, the metallic powder is fed through nozzles near the laser in such a way that when a melt pool is formed on the part, the powder is added and forms a new layer. Layer size can range from 500µm to 1000µm [2]. Compared to LS (50µm to 100µm), the thicker layers significantly reduce build times. However, they also lead to poor surface finish, and limit ability to produce complex designs.

Powder Bed Fusion

Electron Beam Powder Bed Fusion (EPBF) and Laser Powder Bed Fusion (LPBF) are each metal powder bed fusion technologies. In each of these processes, the feedstock material is a metal powder. A small layer of the powder is spread over the build plate, an energy source traces the cross section of the part according to the digital part file, and the build plate lowers to accommodate the next layer of powder. The process repeats until the entire part is produced. The two processes differ in the energy source they use to melt the metal powder.

Electron Beam Powder Bed Fusion

In this process electrons travel at high speeds towards the powder layer. The EPBF machine emits electrons from a cathode. A vacuum is required to allow the charged particles to maintain enough kinetic energy to melt the powder particles. A magnetic field can steer the particles to trace the part cross section. The electron beam efficiently transfers this kinetic energy to the powder. The powder used in EPBF machines is larger than that used in LPBF. Similarly, powder layer thickness is also greater. This results in higher build rates than LPBF.

The electron beam is focused in order to fully melt the powder. Before this step, a defocused beam sinters the powder layer for two important reasons. First, this improves conductivity of the powder bed. Second, the difference in charge could disrupt the powder layer if the powder particles are not partially bonded together. When the part is complete, the sintered “cake” must be removed by blasting it with a media, often the same powder used to build the part. Any cavities in the part must be accessible by the powder gun in order to be removed and reclaimed.

Laser Powder Bed Fusion

In this process, a laser beam, often generated from CO_2, Nd:YAG, or Yb, of infrared or near infrared wavelength is focused through a lens and directed towards the build area using mirrors. When the photons reach the powder, only portion of their energy is transferred in order to melt the powders. A portion of the photons’ energy is reflected away from the surface. This portion is related to the material property, absorptivity. This fact, in addition to the lower power of the laser compared to an electron beam, limits the material deposition rate. The powder diameter and powder layer heights are smaller in the LPBF process, this results in a smaller minimum feature size and improved surface finish.

Unlike the electron beam process, sintering the powder bed with a defocused beam is not necessary. Enclosed spaces only require an opening large enough to shake and pour the unmelted powder out. However, media blasting all surfaces is beneficial for several reasons. First, it improves the surface finish,

potentially minimizing irregularities that could increase stress locally. Second, the surface becomes work hardened with compressive residual stresses that resist surface cracks from opening.

Additive Materials

Material selection is limited for applications involving AM. The rate at which the metal solidifies can be an order of magnitude greater than traditional casting methods [1]. Titanium alloys are popular because they have great mechanical properties and resistance to oxidation. One factor that limits the use of titanium is its great cost compared to steel or aluminum alloys. However, in additive manufacturing, there is little wasted material, therefore a low buy-to-fly ratio, which reduces the effective cost of the material. Nonetheless, researchers are searching for aluminum and steel alloys which are capable of regularly producing parts with acceptable shape, grain structure, and strength. The alloys known as weldable alloys have been successful. AlSi10Mg is currently the most commonly used aluminum alloy in additive manufacturing, more specifically in LPBF process. The alloy has traditionally been used in casting applications due to its relatively low coefficient of thermal expansion (CTE) resulting in lower residual stresses and lower chance of hot cracking or hot tearing due to the addition of silicon. Additionally, increasing the composition of silicon and magnesium reduces the difference in temperature between the liquidus and solidus temperatures thereby reducing the chances of hot tearing.

Table 1 Mechanical Properties of Common AM Alloys and Al 6061-T6[3]–[5]

Mechanical Properties	AlSi10Mg (annealed 2 hours @ 300˚C) [3]	Aluminum 6061-T6 [4]	Arcam Ti6Al4V [5]
Tensile Strength	345 MPa	310 MPa	1020 MPa
Tensile Strength (z-direction)	350 MPa		
Yield Strength	230 MPa	276 MPa	950 MPa
Yield Strength (z-direction)	230 MPa		
Modulus of Elasticity	70 GPa	68.9 GPa	120 GPa
Modulus of Elasticity (z-direction)	60 GPa		
Elongation	12%	18%	14%
Elongation (z-direction)	11%		
Fatigue (z-direction)	97 MPa	96.5 MPa	600 MPa

The above table shows that while the titanium alloy is significantly stronger than the two aluminum alloys, the differences are not as great between the high strength engineering alloy Al 6061-T6 and the castable and recently successfully sinterable AlSi10Mg. Notable differences being Al 6061-T6 is more ductile and has a lower ultimate tensile strength.

Properties

Additively manufactured components are likely to have a more irregular surface compared to machined components [6]. This impacts the design of internal channels such as those found in a hydraulic manifold. A group of PhD candidates, a professor, a postdoctoral researcher, and other researchers for the Center for Human Robotics, Istituto Italiano di Tecnologia, produced several cylindrical samples and varied the angle between their axis and the build plate in order to analyze the influence overhang angle has on surface roughness, especially unsupported surfaces such as those within internal channels. Additionally, the group produced samples in both AlSi10Mg and Ti6Al4V in order to compare results from different the materials.

There are many ways to describe the roughness of a surface. First, the arithmetic mean roughness (R_a) is the average of the absolute values of height. Second, the maximum height profile (R_z) is the distance from profile height to valley depth of an individual sample. Third, the maximum measured height profile (R_{max}) is the largest of the individual height profiles. These three measurements were used to characterize the different samples [6]. The results show that the surface roughness is dependent on build angle. The lower build angles have rough particles on the surface with the upper, unsupported surface rougher than the bottom. When the build angle reaches 60 degrees, the roughness decreases, and the upper surface now is less rough. Lastly, the titanium samples were measured less rough than the aluminum samples.

Design for Additive Manufacturing

It is important to consider the form, fit, function, and process of manufacturing the component from design inception, through fabrication, and post-processing. In order to gain the maximum potential from additive manufacturing, each step must take advantage of additive manufacturing.

Internal channels

The hydraulic manifold is key to controlling hydraulic actuators. Hydraulic fluid is directed through the manifold to the control valve, then to the actuator, and back through the valve and the manifold to the tank to be pumped through again. These networks of internal channels can be complex and result in many minor losses between the pump and the tank. Products manufactured using LPBF can include internal channels that follow optimized paths that are impossible to machine using traditional manufacturing techniques. The loose powder can then be shaken loose from these channels.

Integrated structural and non-structural components

Part count reduction is one of the major benefits of AM. Structural components such as a robotic arm manufactured to include the internal channels of its own hydraulic manifold automatically reduces the part count by at least one. The complex geometries of the integrated parts can be printed as designed in CAD without additional labor of bonding or finishing interfacial surfaces.

Light weighting

Adding material layer-by-layer enables the removal of material in the design process. A complex internal structure such as a lattice can have a very high strength-to-weight ratio. The lattice's density can be specifically altered to give regions the exact amount of support they need while the void space saves weight from the final part.

Hydraulic Theory

The way hydraulic systems effectively transfer a force from one point in the system to another is explained by Pascal's law. These systems enclose relatively incompressible fluid, and so by Pascal's law, a pressure change in one location is simultaneously exerted through the entire system. For example, when a pump changes the pressure in one location, a piston in another location extends due to the pressure acting on the cylinder. The rate of piston movement and the force that can be exerted are related to the flow rate of the pump, the pump pressure, and the area of the piston bore.

Components (Actuators, Valves, Manifold)

Figure 1 below depicts a hydraulic system including a double acting cylinder. A 4-way directional control valve directs pressurized fluid to one side of the piston, causing the piston to either extend or retract. Fluid can also be locked inside the piston; in which case the piston does not move and the fluid on the

positive pressure side of the pump is returned by way of the pressure relief valve. The control of a loader arm combines two of these double acting cylinder systems as seen in Figure 2.2.2.

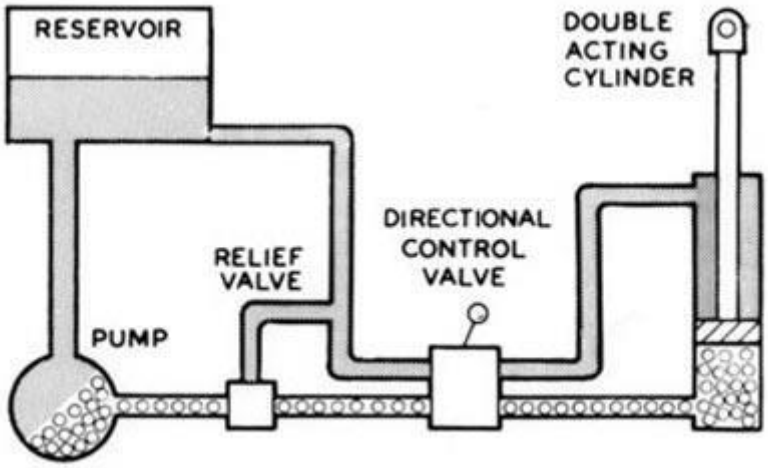

Figure 1 Hydraulic System using Double Acting Cylinder. Cross Manufacturing.

The system described above is an open center system due to the oil flowing through the control valve back to the tank. Most systems are this type. Closed center systems use control valves with the inlet port blocked and variable displacement pumps. With the control valve in neutral, the pump is "de-stroked" to zero flow. These fixed displacement pumps are less expensive than the variable displacement pump used in a closed center pump. However, the closed center system is often more efficient because the oil is not pumped through the valve when not in use.

Traditional Hydraulic Manifold

Manufacturing Methods (Laminar manifold, drilled block)

There are two traditional methods of manufacturing hydraulic manifolds, laminar and drilled block. This section will describe each method and their associated strengths and weaknesses as components in hydraulic systems.

Laminar Manifold

The laminar manifold is named after its many layers that make up the component. Thin plates, typically made of steel, are milled in such a way that when layered on top of each other, they produce channels through the component. The layers are then braised together and finished with a plate on either side. The completed part can contain pressures as high as 10,000 psi and internal channels are smooth because of the layer-by-layer machining process. This method requires a completely custom designed and cannot be easily modified to fit future designs.

Drilled Block Manifold

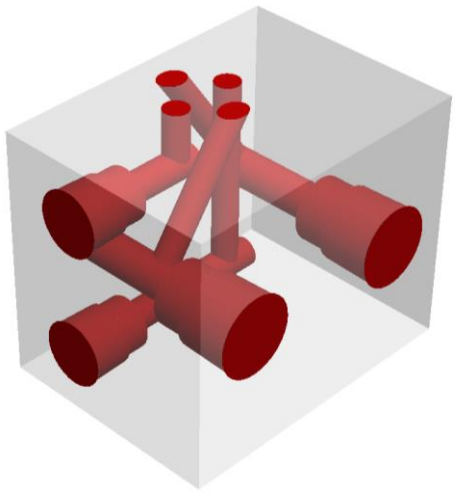

Figure 2 Model of traditional drilled block manifold.

A drilled block manifold is manufactured exactly as it sounds. Depicted in Figure 2, a block of metal, typically made of aluminum, steel, or iron is drilled to contain several passages. These drilling operations must be straight into and out of one of the blocks surfaces. If a passage must turn within the component, an additional drill hole must be made and then capped at the surface. Passages can also be interconnected with the use of a cartridge valve inserted into the manifold through a valve cavity. These drilled block manifolds inherently have excess material because they need several passages that do not intersect and are limited to straight lines.

Prior Work using Additive Manufacturing

A journal article from 2018, published by a group from Dalian University of Technology, describes their efforts to automate the design of a hydraulic manifold specifically for additive manufacture [7]. The group first analyses the traditional hydraulic manifold and presents three ways performance and reliability are limited by traditional designs. Traditional hydraulic manifolds inevitably have right-angled corners, process cavities, sudden changes in radius, for the channels to avoid intersecting. First, these features cause a pressure drop that could be avoided by smoothing transitions. Next, these features cause turbulence, leading to inaccuracy in sensors and degrade the component through cavitation. Lastly, they lead to increased temperatures in the component and in the fluid. They compared the theoretical pressure drop of traditionally manufactured channel geometries and similar channels modelled for additive manufacture, leading in some cases to a 75% reduction in fluid resistance.

In 2012, an F1 engineering team, Red Bull Technology, published a report describing their experimentation with the Direct Metal Laser Sintering (DMLS) of Titanium (Ti6Al4V) for the application of redesigning a hydraulic manifold [8]. They produced several test specimens of various cross sections and wall thicknesses. Each exposed to a standardized testing procedure of including sustained periods of high temperature and pressures. It was determined even the specimen with the thinnest walls (0.5mm) was still acceptable. Additional tests were conducted to compare flow velocity of traditional monoblock manifolds to the internal channels only additive manufacturing can produce. The results showing that fluid flow velocity could be increased up to 250%. This suggests that significant reductions in energy losses are possible, thereby reducing necessary energy input from an engine or battery per energy out.

A group from the Center for Space Human Robotics describes their redesign of a hydraulic manifold for its use in a quadruped robot [9] and reference results in the article by Red Bull Technology. This group claims to be the first to design a hydraulic manifold to be produced by DMLS using an aluminum alloy (AlSi10Mg). The group chose to use aluminum instead of titanium for several reasons, including lower cost, higher thermal conductivity, lower theoretical density, and easier to post process.

Included in Solid FreeForm Fabrication 2017: Proceedings of the 28th Annual International Solid FreeForm Fabrication Symposium – An Additive Manufacturing Conference, members of the Naval Research Laboratory published the results of their design, fabrication, and qualification of a quadruped body constructed using DMLS in aluminum [10]. The frame is constructed of three printed parts, two symmetric, and integrated within it is the hydraulic manifold to distribute pressurized fluid to the control system for each of the four legs. This report is very detailed with respect to the design of the components, including determining channel cross sections, the post-processing of the components, including how to finish the surface inside the channels, and the methods of analyzing the finish part.

Performance metrics

The traditional manufacturing method of a hydraulic manifold involves drilling, expanding, and reaming the passageways through a billet of steel or aluminum alloy as described before. The resulting right-angle corners, cavities, and sudden changes in radius theoretically cause pressure loss and temperature rise [11]. This increases the cost of operation because more powerful pumps are required for the same output at the work section and increased temperatures decrease the service life of the fluid.

Pressure Loss

The theoretical pressure drop described above is explained by the fluid dynamics concept of head loss and the resulting reduction in input power according to thermodynamics [11]. Head losses are pressure drops within a control volume and are indicative of the mechanical energy of the fluid converting into thermal energy. This is due to the fluid passing through bends, junctions, etc. which result in churning rather than straight flow paths. Each of these bends or junctions has a corresponding head loss coefficient, described in detail within comprehensive collections based on decades of experimental data. In Table 2, examples and corresponding loss coefficients are listed. As a result of the limitations of traditional manifold manufacturing methods, several of these examples make up channel, often with a dozen or more channels per manifold. This can lead to significant head loss and therefore require higher input pressure and more powerful pumps.

Table 2 Loss coefficients of various bends and junctions

Component	Loss Coefficient
Regular, 90˚ Bend	0.3
Long, 90˚ Bend	0.2
180˚ Return Bend	0.2
Tee, Line Flow	0.2
Tee, Branch Flow	1.0

Temperature Rise

The rise in temperature due to the churning whirlpools results in several many other problems for the system. Firstly, a common hydraulic fluid, mineral oil, has been shown to have reduced service life due to

increased temperatures [7]. It is stated that there is a 90% reduction in service life for each increase of 15˚C. Additionally, the fluid becomes less viscous and loses lubricating performance at higher temperatures, both leading to leaks due to the system being under high pressure. Finally, the hydraulic manifold is not intended to act as a heat exchanger, though increased fluid temperatures within will increase the temperature of the manifold, therefore causing the part to expand and contract if the system is turned on and off. The repeated stressing of the component and neighboring components is likely to lead to failure.

Lightweighting

The process of melting metal powder layer-by-layer enables the design using volume lattices that are strong but also light. These structures are often impossible to machine with subtractive manufacturing methods, though they be produced easily using additive manufacturing. Additionally, the density of these lattices can be altered relative to the load experienced by adjusting the node spacing or cross member thickness based on simulation data.

Application

The goal of this project is to design a robotic arm using additive manufacturing. Additive manufacturing enables many design freedoms that are potentially beneficial for robotic devices such as those carried to space for remote exploration. In this application, space and weight savings as well as energy efficiency are very valuable to the companies transporting these robots to space.

For reference, the rover arm (also called the instrument deployment device or IDD) used on NASA's Mars Exploration Rovers has been analyzed for successful scale and load bearing characteristics of a robotic arm for this application. This design will differ from the arm used on Mars Exploration Rovers in the past because it will be controlled with hydraulic actuators. Hydraulic actuators have tremendous power density compared to electric motors. Additionally, this design will differ from other robotic arms by including the hydraulic lines and housings for control valves into the structural members of the arm. This component, called the hydraulic manifold, will essentially be eliminated as it is manufactured out of the same material already being used for the arm itself.

On the following page, Figure 3 shows a partial assembly of components making up a robotic arm and highlights the section of arm designed as part of this report.

Figure 3 Model assembly of robotic arm.

Design Requirements

- Internal Channels
- Load Capacity: 10kg or at least 50% of the arm's mass at full extension of the arm

Functional Requirements

- Mobility Range: 1m
- Mass: Approximately 20kg, including structural members, actuators, valves, etc.

Design, Fabrication, and Post-processing of the Manifold

The design of a robotic arm specifically for additive manufacturing considers the design itself, the manufacturability, and the post-processing steps needed to achieve a successful component. Many of the steps in this process are specific to additive manufacturing and may not simply be adapted from traditional, subtractive engineering processes.

Design

Major support for additive manufacturing surrounds the ability to place material exactly where it is necessary. This not only reduces part weight, but greatly improves buy-to-fly ratios because unmelted powder, following the build process can be recycled and used again. Many turn towards topology optimization tools to design for minimum material or specified strength to weight ratio. Loading conditions, minimum wall thickness, and preserved regions are some of the inputs the designer provides to enable the computer to optimize material usage.

Fabrication

It is important to note, that the optimal geometry is not necessarily the one with the least material in the finished part. The designer must consider where support structures are necessary at this stage because they represent one of the most wasteful uses of material in additive manufacturing. Unlike unmelted powder, support structures are not easily recycled, similar to the chips resulting from subtractive

manufacturing methods. In many cases, part orientation or geometry can be slightly altered, and the amount of support structures can be reduced or eliminated.

Post-processing

The as-printed component is very close to the final part. However, there are several important post-processing steps that must be completed before the final part is satisfactory. First of all, if additional support material is necessary in the fabrication step, this must be removed by means of prying, sanding, or machining it away. Unlike unmelted powder, it is very costly to return this material to a useable state for metal additive manufacturing. Additionally, this additional step requires additional time which adds cost to the total production cost of the part. This is why the design of the part itself must be self-supporting when possible to limit the amount of additional support material and the expense of removing this material. Likewise, when producing internal channels, such as those in the hydraulic manifold, it is necessary that the channels themselves are self-supporting because it is not possible to access these surfaces to remove the support material. Additionally, the unmelted powder which remains in the channels after fabrication must be removable by shaking or by flushing them out in order for them to be usable. Second, the surface roughness of an additively manufactured component is generally not as good as a machined part. The melt pool can pick up unmelted powder at its edge and the resulting surface has many irregularities. In the structural members of a robotic arm, these irregularities can initiate a crack due to stress concentration. The outer surface of the component is treated by shooting the same powder through an air gun to both knock away loosely held powder particles and induce compressive residual stresses which tend to resist crack initiation and propagation. This step is combined with reclaiming the unmelted powder for reuse. The internal surfaces are important for the efficiency of the system during operation. Additionally, if any loosely held particles dislodged during operation, this could potentially damage the equipment attached to the component such as pumps, actuators, or sensors. As stated above, the channels must be flushed to pick up any particles with the potential of dislodging from the surface. Additionally, reducing the surface roughness will reduce the pressure drop of the component, thereby reducing the power required to operate the system.

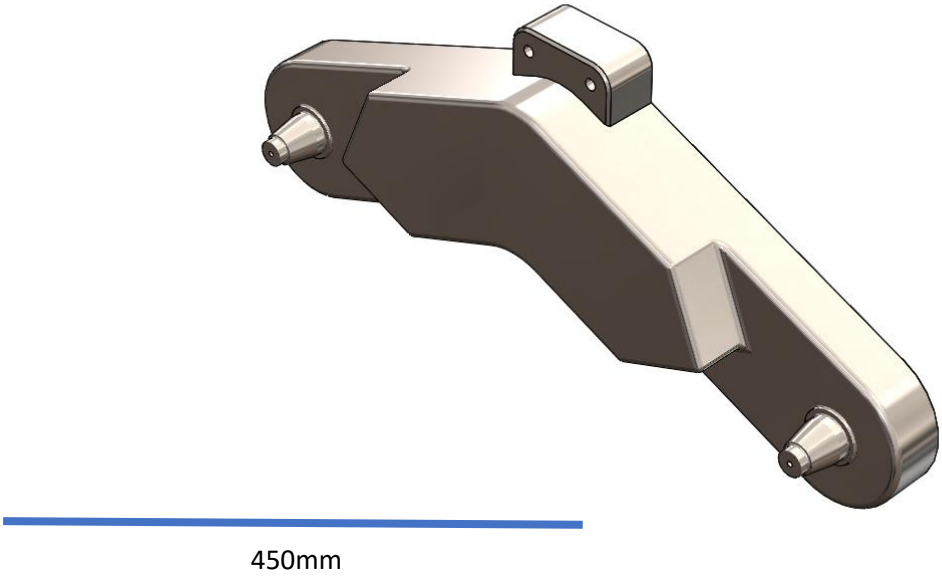

Figure 4 Model of the robotic arm.

The design for this member of the arm, shown in Figure 4 above, includes stub axles on either end and two mounting locations for the hydraulic cylinders used to move the arm. The part is intended to be oriented such that there is no overhanging material so no support material is necessary. The large center region houses the hydraulic manifold for the two hydraulic cylinders. The large cross section will provide lots of stiffness and does not require full infill. Instead, this region is intended to be solid only near the outer surface and the surfaces of the internal channels. Then, the remaining volume can be filled with a volume lattice to keep the part strong but lightweight.

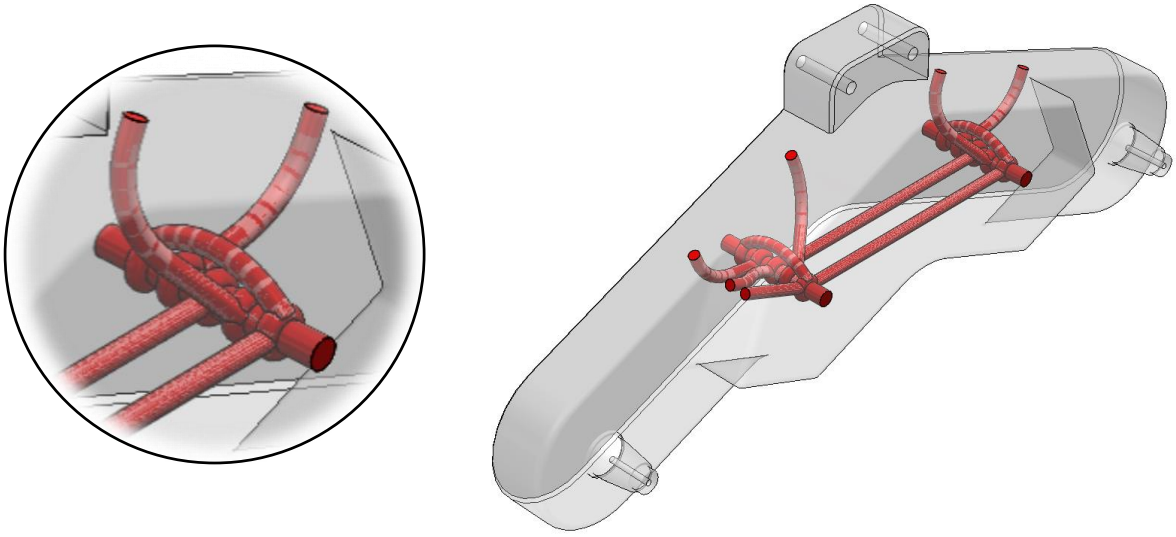

Figure 5 (a.) left, Enhanced view of spool-type directional control valve. (b.) right, Robotic arm with internal channels.

The internal channels of the hydraulic manifold direct the hydraulic fluid from the pump to the control valve, to the hydraulic actuator. Figure 5 above shows the internal channels which have been designed to have no sharp bends (less than 5 times the diameter of the channel). The channels meet at a spool-type directional control valve. This design was chosen in order to limit the losses in the hydraulic system. The losses will be tested using a testing apparatus designed as part of this project.

Testing Apparatus – Design and Construction

In this application, it is important to maximize the productivity of the fluid. The power of the pump produces a pressure differential in the fluid between its inlet and outlet. Then a series of junctions, constrictions and valves direct the fluid to the cylinder or motor being powered. Each of these contributes to major and minor losses of energy in the system. Viscous effects of the fluid and roughness of the pipe wall cause frictional energy losses, and these are referred to as major losses. Any energy loss in addition to that resultant from a similar length of straight pipe are referred to as minor losses. These minor losses can result from bends, junctions, changes in cross sectional area, etc. The hydraulic manifold naturally has many junctions and changes of direction in order to control a hydraulic actuator's motion. Maximizing the productivity of the fluid involves optimizing the network of channels and valves in order to limit unnecessary losses between the pump and the actuator.

Objective

The objective of this experiment is to investigate the pressure drop in each of the hydraulic manifold designs, a traditional block manifold and an integrated manifold design, and to determine the power savings from the improved design. This experiment will provide quantitative evidence to support or oppose the energy saving benefit of designing a hydraulic manifold for additive manufacturing. The greater the reduction in pressure drop, the greater the energy savings potential. After all, greater the pressure drops the greater the amount of unnecessary work done by the pump in order to do the same amount of work by the actuator.

Method

The manifold blocks are connected in series to ensure testing occurs using identical flow rates. On the following page, Figure 6 depicts the apparatus used to test the pressure drop of two manifolds, A and B, simultaneously. At the inlet and outlet of each manifold, a pressure tap (a tee union in the connecting hose) leads to a water column to measure pressure head at each location. The outlet of the first manifold and the inlet of the second manifold will have a shared pressure tap for a total of three measurement locations. The height of each of these water columns, Z_{A1}, Z_{A2} & Z_{B1}, and $Z_{B2,}$ will be measured from the tee union. On the following pages, the calculations to find pressure drop from the heights of these water columns will be explained.

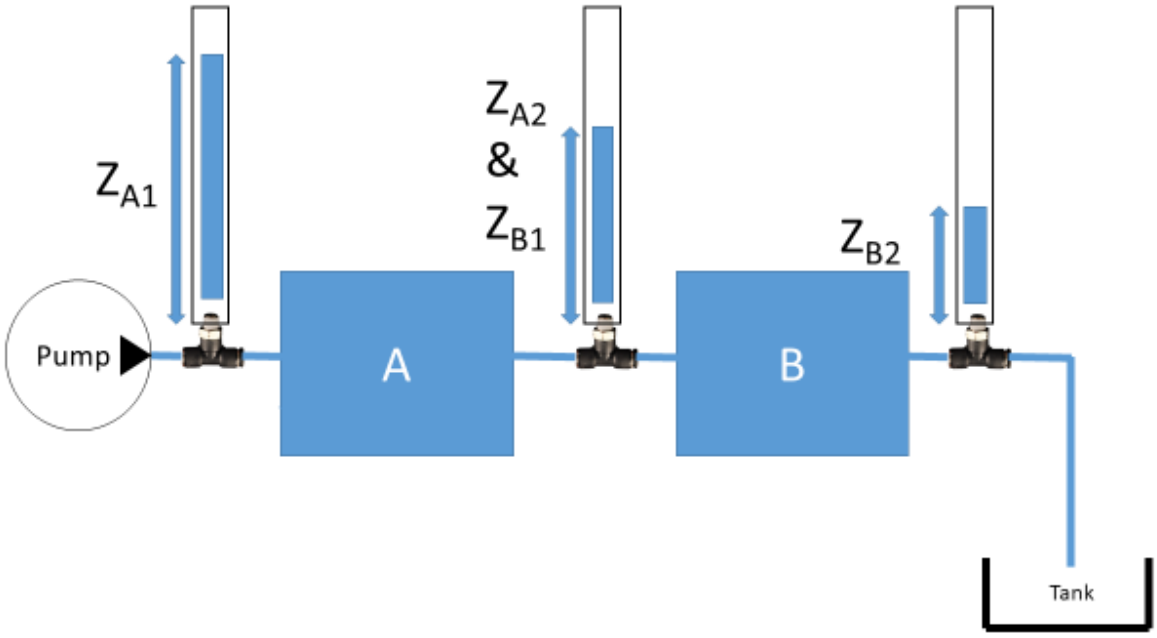

Figure 6 Diagram of pressure drop testing apparatus.

Sufficient time must be allowed for the system to reach steady state. At that point, the water column should have virtually no flow in or out and any air should be pushed out of the system. The order the manifolds are attached in series is not critical to the results. Lastly, the flow rate should be adjusted in order to be representative of Reynolds number of the final system.

Theory

This experiment will use water as the working fluid because it is readily available and easy to clean up. The relationship between Reynolds number, characteristic length, a value constant with geometry of the part, and kinematic viscosity, a parameter of the fluid, and a given velocity for the final system, we may calculate the flow rate that will ensure appropriate testing conditions.

Reynolds number is defined as the ratio of inertial forces to viscous forces and can be expressed as:

$$Re = \frac{\rho v d}{\mu} = \frac{v d}{V}$$

v: Velocity of the fluid
d: Characteristic length – diameter of the channel
ρ: Density of the fluid
μ: Dynamic Viscosity of the fluid
V: Kinematic Viscosity of the fluid

On the following page, Table 3 shows values for kinematic viscosity of several grades of hydraulic oil and water which can all be found at engineeringtoolbox.com.

Table 3 Kinematic viscosity of various grades of hydraulic oils and water

ISO Grade	Equivalent SAE Grade	Kinematic Viscosity [cSt]	
		313K	373K
32	10W	32	5.4
46	20	46	6.8
68	20W	68	8.7
100	30	100	11.4
150	40	150	15
220	50	220	19.4
Water		0.6591	0.2938

The hydraulic fluid chosen for the final application is one that is ideal for smaller mobile equipment such as a robotic arm. Liquid Wrench powered by EnviroLogic Mobile Equipment Hydraulic Fluid is readily biodegradable and safe for use in ISO 46 grade hydraulic systems. Therefore, the following calculations describe the calculation of flow rate required for the experiment based on the temperature of the working fluid.

$$Re_{water} = Re_{hydraulic}$$

$$\frac{v_{water} d}{V_{water}} = \frac{v_{hydraulic} d}{V_{hydraulic}}$$

$$v_{water} = \frac{V_{water}}{V_{hydraulic}} v_{hydraulic}$$

The suggested fluid velocity for this system with hydraulic fluid is 15 ft/s or approximately 4.572 m/s.

Therefore, the following chart calculates the appropriate fluid velocity for this system with water as the working fluid. The chart shows that as temperature increases, the ratio of kinematic viscosity changes such that velocity must increase as well. Finally, the flowrate can be calculated according to the following relationship:

$$Q = v \frac{\pi d^2}{4}$$

By measuring a sample of the working fluid at the entrance and the exit of the system, after running at steady state, the average temperature is calculated. Then, the fluid is caught as it pours out of the system, and the mass of the captured fluid is recorded, the mass flow rate can be quickly converted to volume flowrate, and the inlet flow can be adjusted to reach the goal.

Measuring pressure with a water column

First, Bernoulli's Principle states that the sum of the pressure energy, the kinetic energy per unit volume, and the potential energy per unit volume of at any point along a streamline is equal to the sum of those energy terms plus the head loss along that streamline to another point in the control volume.

In this case we are considering a tall cylindrical column of water. At steady state, velocity is constant and zero at all points in the column, therefore friction by viscous forces is negligible. Also, the density of the fluid can be considered constant and the flow incompressible. Now, we may consider the energy equation below:

$$\frac{P_{in}}{\rho} + \frac{{v_{in}}^2}{2q} + z_{in} = \frac{P_{out}}{\rho} + \frac{{v_{out}}^2}{2q} + z_{out} + h_L$$

As stated above, the velocity is zero at all points in the water column:

$$v_1 = v_2 = 0\,{}^{m}/_{S}$$

The origin in the z-direction is located at the base of the water column. Therefore, this term on the left side will cancel out.

$$z_1 = 0\,m$$

Finally, location 2 is at the surface of the water column. And so, the gauge pressure at this point must be zero because it is equal to atmospheric pressure.

$$P_2 = 0\,atm$$

The resulting form of the Bernoulli equation can be seen below:

$$P_1 = \rho g z_2$$

Results

Pressure loss testing

Both the novel hydraulic manifold design and a representation of a traditional hydraulic manifold were tested in series. The novel design is in the "A" position pictured above and the traditional design is in the "B" position. The result of running water through the system at the appropriate flow rate Table 4..

Table 4 Height of water columns in pressure loss testing

Za1	1.50m
Za2 (Zb1)	0.38m
Zb2	0.10m

According to the relationship from the Bernoulli equation above, the pressure drop across these manifolds is determined from the height difference of the water columns at the entrance and the exit of the hydraulic manifolds. The results of this calculation are listed in Table 5.

Table 5 Pressure drop of the novel & traditional hydraulic manifolds

	Height difference	Pressure drop
Za1-Za2	1.12m	10.98kPa
Zb1-Zb2	0.28m	2.75kPa

This result was not as expected. The prototype was cut open in order to examine the quality of the printed part and look for potential factors contributing to the much greater pressure drop. In hindsight, it is likely this region in the directional control valve, pictured in Figure 7(a.) which causes the fluid to loose pressure. The area the fluid flows through increases and decreases, causing the flow to accelerate. This results in energy losses in the fluid and pressure drop. Additionally, in Figure 7(b.), the top view of the valve in the upper right shows that the polymer filament may have bridged across this gap causing more resistance to this flow.

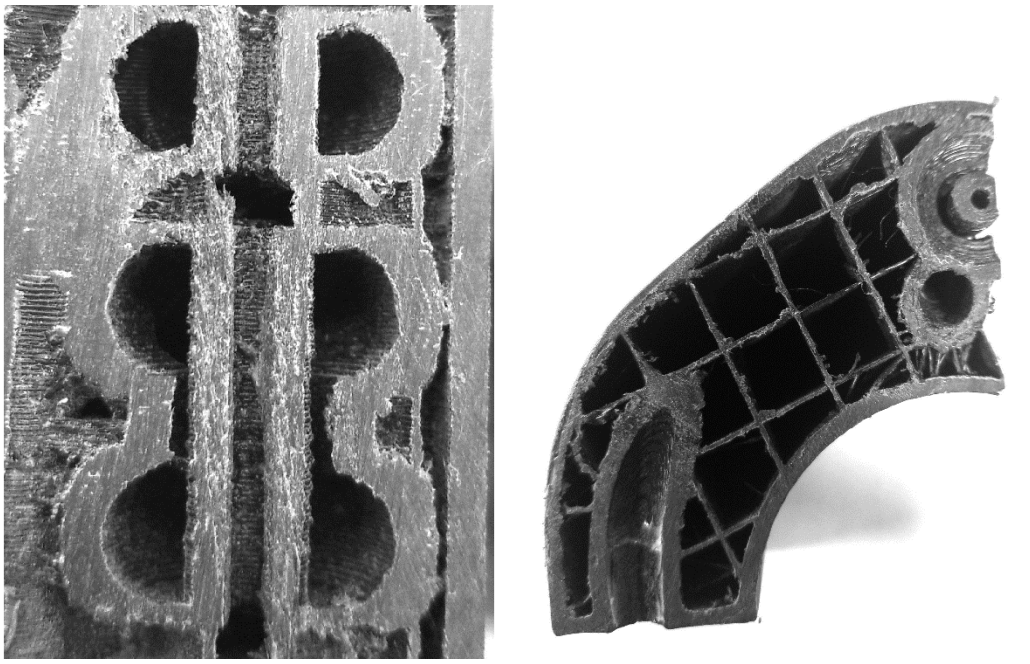

Figure 7 (a.) left, Cutaway of the spool-type directional control valve. (b.) right, Cutaway showing internal channels and DCV.

Simulation stress analysis

The SolidWorks simulation tool was used to estimate the static loading of the structural member. The loads were estimated using the goal length (1m) and load capacity (10kg) of the arm and the estimated mass of the arm and other components (20kg). As seen in Figure 8, the location with the greatest stress is the base of one of the stub axles. Deformation is exaggerated in this model. The magnitude of the stress in this location is well below the yield strength of the material, Ti6Al4V, with a factor of safety of 36. Clearly, when the arm is in motion, the stress is not a static load and will likely be greater based on the acceleration of the arm. This acceleration must be limited so that the stress induce will not be too great.

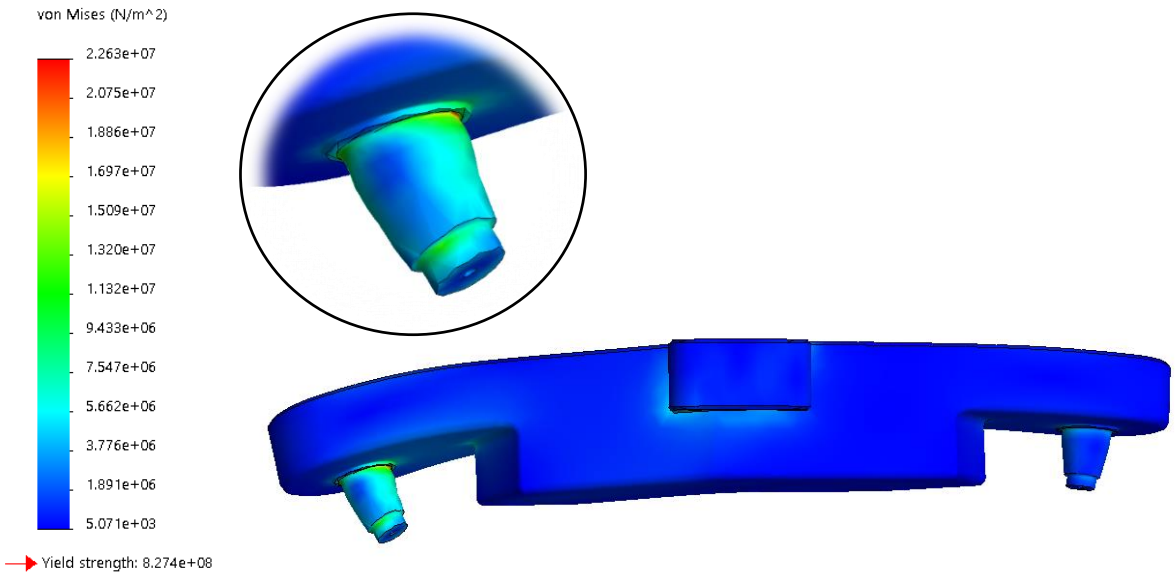

Figure 8 Solidworks static stress simulation.

Conclusion

This project provides a starting point for further exploration into Design for Additive Manufacturing. It has been shown that the two components can become integrated to potentially provide a lighter weight and more efficient design for robotic arms. Though the results from the pressure loss testing were not as expected, the procedure and apparatus developed will be applicable to future development and can be used to compare two different designs simultaneously or determine the pressure drop of a single manifold.

Recommendations and Future Work

The scope so far has been limited to just one of the structural members of the robotic arm but can be expanded in the future to include other components and the hydraulic system itself. There are many features which are particularly relevant to additive manufacturing including the internal channels and potentially a volume lattice or topology optimization. Such autonomous design programs could potentially produce a significantly different, organic design. Additionally, as additive manufacturing develops, the conceivable designs will grow as those designs which were previously impossible to produce become possible. It will also be exciting if future groups can use metal AM equipment to produce prototypes of this design.

Acknowledgements

I would like to thank Professor Narra for her support and encouragement through the conception, progression, and completion of this project. I am grateful to have her to advise me on this project and through my senior year at WPI.

I also received help from Professor Daniello at WPI in order to design the pressure drop testing apparatus. He was a great help with this and guided me towards a simple yet accurate design.

I would also like to thank WPI and the mechanical engineering department for many great years. This project has been a great experience and an opportunity to put several years of theory into practice.

References

[1] D. D. Gu, W. Meiners, K. Wissenbach, & R. Poprawe, and R. Poprawe, “Laser additive manufacturing of metallic components: materials, processes and mechanisms Laser additive manufacturing of metallic components: materials, processes and mechanisms,” *Int. Mater. Rev.*, vol. 57, no. 3, pp. 133–164, 2017.

[2] B. Dutta and F. H. Sam Froes, *The additive manufacturing (AM) of titanium alloys*. Elsevier Inc., 2015.

[3] Arcam, “Arcam -Ti6Al4V Titanium Alloy Powder,” pp. 4–6, 2020.

[4] EOS GmbH - Electro Optical Systems, “EOS Aluminium AlSi10Mg,” *GPI prototype Manuf. Serv.*, vol. 49, no. 0, pp. 1–5, 2014.

[5] B. Rockwell, “Aluminium 6061 properties,” pp. 1–3, 2020.

[6] J. Pakkanen *et al.*, “Study of Internal Channel Surface Roughnesses Manufactured by Selective Laser Melting in Aluminum and Titanium Alloys,” *Metall. Mater. Trans. A Phys. Metall. Mater. Sci.*, vol. 47, no. 8, pp. 3837–3844, 2016.

[7] M. Ma, H. Zhang, J. Zhang, and C. Wang, “Automatic Design of Hydraulic Manifold Block Based on 3D Printing,” *J. Phys. Conf. Ser.*, vol. 1087, no. 4, 2018.

[8] D. E. Cooper, M. Stanford, K. A. Kibble, and G. J. Gibbons, “Additive Manufacturing for product improvement at Red Bull Technology,” *Mater. Des.*, vol. 41, pp. 226–230, 2012.

[9] C. Semini *et al.*, “Additive manufacturing for agile legged robots with hydraulic actuation,” *Proc. 17th Int. Conf. Adv. Robot. ICAR 2015*, pp. 123–129, 2015.

[10] J. T. Geating, M. C. Wiese, and M. F. Osborn, “Design, Fabrication, and Qualification of a 3D Printed Metal Quadruped Body: Combination Hydraulic Manifold, Structure and Mechanical Interface,” *Solid Free. Fabr. Symp.*, pp. 2447–2466, 2017.

[11] B. Schmandt and H. Herwig, “Internal flow losses: A fresh look at old concepts,” *J. Fluids Eng. Trans. ASME*, vol. 133, no. 5, pp. 1–10, 2011.